

Electroswitchable Photoelectrochemistry by Cu^{2+} –Polyacrylic Acid/CdS-Nanoparticle Assemblies

Laila Sheeney-Haj-Ichia, Zoya Cheglakov, and Itamar Willner*

*The Institute of Chemistry, The Farkas Center for Light-Induced Processes,
The Hebrew University of Jerusalem, Jerusalem 91904, Israel*

Received: August 14, 2003; In Final Form: October 22, 2003

CdS nanoparticles are incorporated into a poly(acrylic acid) (PAA) film associated with an Au electrode, and the nanoparticles are covalently linked to the matrix. Cu^{2+} ions are incorporated into the CdS-nanoparticle–PAA film, and the electroswitchable photocurrent generation by the system, in the presence of triethanolamine as sacrificial electron donor, is demonstrated. The electrochemical reduction of the CdS– Cu^{2+} –PAA state to the CdS– Cu^0 –PAA state (–0.55 V vs SCE) leads to the formation of conductive metal nanoclusters that facilitate electron transfer of the CdS-conduction-band electrons to the electrode, and the generation of the photocurrent. The oxidation of the Cu^0 clusters to Cu^{2+} ions linked to the carboxylate units of PAA (applied potential +0.55 V vs SCE) switches off the photocurrent. The system not only is active for the reversible electroswitchable photocurrent generation but also acts as a photoelectrochemical detector of Cu^{2+} ions.

Introduction

Electrochemical readout of molecular photoswitchable redox-states^{1,2} and of light-switchable bioelectrocatalytic processes³ has been a subject of extensive research efforts directed to the development of optical information storage and processing systems. The reverse optical transduction of electroswitchable redox functions of electroactive molecular⁴ or polymer⁵ films associated with electrodes was reported by the use of surface plasmon resonance spectroscopy. The solvent-controlled switching of the photoelectrochemical functions of semiconductor nanoparticles was recently reported by the immobilization of CdS nanoparticles in an acrylamide film linked to the electrode surface.⁶ The water-swollen state of the polymer results in the dispersion of the nanoparticles in the polymer in a configuration that lacks electrical contact with the electrode, leading to a switched-off photoelectrochemical system. The shrunken polymer generated in the presence of acetone yielded electrical contact between the nanoparticles and the electrode and switched on the photoelectrochemical function of the system. Also, the photoelectrochemical functions of semiconductor nanoparticles were switched on by a biocatalytic process, and switched off in the presence of the enzyme inhibitor.⁷ Recently, Cu^{2+} ions incorporated in an acrylic acid polymer film linked to an electrode were reported as an electroswitchable medium of electrical conductivity.⁸ In the Cu^{2+} –poly(acrylic acid) state the film is nonconductive whereas upon its reduction to the Cu^0 –poly(acrylic acid) state the film revealed electrical conductivity. These properties of the film were used to assemble electroswitchable and tunable biofuel cells.⁹ Here we wish to report on an electroswitchable photoelectrochemical system composed of CdS nanoparticles incorporated in a Cu^{2+} –poly(acrylic acid) film associated with an Au electrode surface.

Metal nanoclusters such as Pt or Au coupled to semiconductor (SC) nanoparticles were reported to promote the photoelectrochemical function of the SC particles.^{10,11} Electron transfer of conduction-band electrons to the metal clusters facilitates the electron–hole charge separation, and the transport of the

electrons to the bulk electrode surface. In the present study, electrogenerated Cu^0 clusters formed in the poly(acrylic acid) (PAA) film facilitate the electron transport from the photoexcited CdS nanoparticles to the electrode support and promote the generation of the photocurrent.

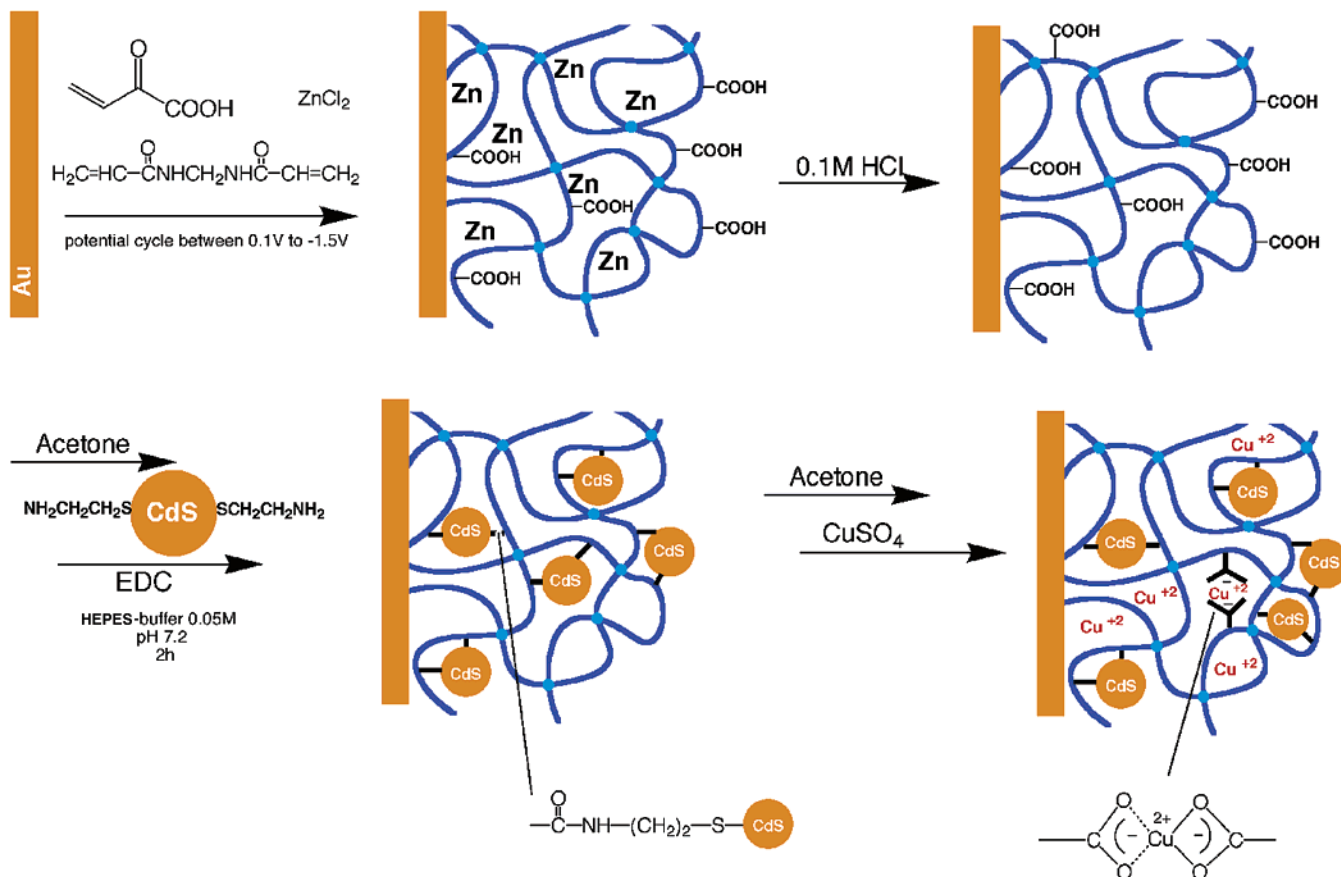
Experimental Section

Photoelectrochemical Measurements. Experiments were performed with a home-built photoelectrochemical system that includes a 300 W Xe lamp (Oriel, model 6258), a monochromator (Oriel, model 74080), and a chopper (Oriel, model 76994). The electrical output from the cell was sampled by a lock-in amplifier (Stanford Research model SR 830 DSP). The shutter chopping frequency was controlled by a Stanford Research pulse/delay generator model DE 535. The photoelectrode consisted of an Au-electrode functionalized with the CdS–PAA– Cu^{2+} film. A graphite electrode was used as a counter electrode, and a saturated calomel electrode (SCE) was used as a reference electrode. The photogenerated current was measured between the working and the counter electrode. The electrolyte solution consisted of 0.02 M triethanolamine in 0.1 M Tris buffer, pH 10.

Electrochemical Measurements. Cyclic voltammetry experiments were performed in a standard electrochemical cell using the functionalized Au electrodes. A conventional three-electrode cell, consisting of the Au electrode, a glassy carbon auxiliary electrode isolated by a glass frit, and a saturated calomel electrode (SCE) connected to the working volume with a luggin capillary, was used for the electrochemical measurements. The potential measured upon cyclic voltammetry is reported vs SCE. The cell was positioned in a grounded Faraday cage. Cyclic voltammetry was performed using a potentiostat (EG&G, model 283) connected to a computer (EG&G Software Power suite 103). The electrochemical measurements were performed in 0.1 M Tris buffer, pH = 5.5 as background electrolyte.

Microgravimetric Quartz Crystal Microbalance (QCM) Measurements. Experiments were performed with a QCM analyzer (Fluke) using Au–quartz crystals (AT-cut 9 MHz). The geometrical area of the Au electrode was $0.2 \pm 0.05 \text{ cm}^2$,

* To whom all correspondence should be addressed. Tel: 972-2-6585272. Fax: 972-2-6527715. E-mail: willnea@vms.huji.ac.il.

SCHEME 1: Assembly of the CdS–Cu²⁺–Polyacrylic Acid Film on an Au Electrode

roughness 3.5. Prior to each measurement the modified QCM crystals were dried under a flow of argon, and the crystal frequencies were determined in air. The surface coverage of the respective component was determined by following the frequency change of the crystals upon the stepwise assembly of the different component. The surface coverage was estimated using the Sauerbrey equation,¹²

$$\Delta f = 2f_0^2 \frac{\Delta m}{A(\mu_q \rho_q)^{1/2}} \quad (1)$$

where Δm is the mass change, f_0 is the resonance frequency of the quartz crystal, A is the piezoelectrically active area, ρ_q is the density of the quartz ($2.648 \text{ g}\cdot\text{cm}^{-3}$), and μ_q is the shear modulus ($2.947 \times 10^{11} \text{ dyn}\cdot\text{cm}^{-3}$) for AT-cut quartz.

Preparation of CdS Nanoparticles.¹³ An AOT/*n*-heptane water-in-oil microemulsion was prepared by the solubilization of 2.5 mL distilled water in 100 mL *n*-heptane in the presence of 7.0 g of the AOT surfactant (dioctyl sulfosuccinate sodium salt). The resulting mixture was separated into 60 and 40 mL of reverse-micelle subvolumes. Aqueous solutions of $\text{Cd}(\text{ClO}_4)_2$ (0.24 mL, 1 M) and Na_2S (0.16 mL, 1 M) were added to the 60 and 40 mL subvolumes, respectively, and the two solutions were mixed and stirred for 1 h to yield the nanoparticles. For cysteamine-stabilized CdS nanoparticles we added to the resulting mixture an aqueous solution of 2-aminoethanethiol (cysteamine 0.33 mL, 0.33 M) and 2-mercaptoethanesulfonic acid (0.2 mL, 0.33 M) and the mixture was stirred for 24 h under Ar. Pyridine, 20 mL, was added to the solution, and then the solution was centrifuged and washed with *n*-heptane, acetone, and methanol.

Preparation of Cu²⁺–CdS–PAA Composite on Au Electrodes. Borosilicate glass supports ($22 \times 11 \times 1.1 \text{ mm}$) covered

with a Cr thin sublayer ($2.5 \pm 1.5 \text{ nm}$) and a polycrystalline Au layer ($250 \pm 50 \text{ nm}$) supplied by Arrandee Precious Metal were used as conductive supports. Au-electrodes were modified with poly(acrylic acid) thin film using the reported electropolymerization method.¹⁴ The electropolymerization was performed in an aqueous solution composed of acrylic acid, 2 M, methylenebis(acrylamide), 0.04 M, and ZnCl_2 , 0.2 M, pH = 7.0, upon application of five potential cycles ($50 \text{ mV}\cdot\text{s}^{-1}$) between +0.1 and –1.5 V. The polymer-modified electrode was reacted with 0.1 M HCl for 2 min to dissolve residual amounts of metallic zinc, and then the electrode was washed with water and ethanol to clean the modified surface from Zn^{2+} ions and the excess of monomers. Incorporation of the CdS nanoparticles in the polymer film was accomplished by allowing the acetone-shrunk film to swell in 0.05 M HEPES buffer, pH = 7.2, that contained the cysteamine-functionalized CdS nanoparticles ($2 \text{ mg}\cdot\text{mL}^{-1}$) for 5 min. The resulting film was washed with water and further allowed to shrink by its immersion in acetone. The CdS nanoparticles were further introduced into the polymer film using five CdS “breathing-in” cycles that involve the repeated swelling of the film in the CdS-nanoparticle solution and its shrinking in the acetone. Subsequently, acetone-shrunk film was swollen in a solution of 0.05 M HEPES buffer, pH = 7.2, that included 1-ethyl-3-[3-(dimethylamino)propyl] carbodiimide (EDC) as a coupling reagent for 2 h to couple the nanoparticles to the polymer matrix. The incorporation of Cu^{2+} ions into the CdS/PAA composite was accomplished by using five “breathing-in” cycles, using a solution of CuSO_4 .

Results and Discussion

Scheme 1 depicts the method used to assemble the functional electrode. The PAA film was generated on the Au electrode by

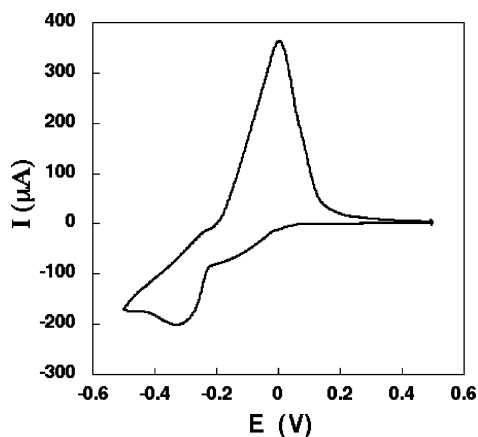


Figure 1. Cyclic voltammogram of the Cu^{2+} -PAA film assembled on an Au electrode. The electrolyte solution consists of 0.1 M Tris buffer, pH = 5.5, under argon, potential scan rate $3 \text{ mV}\cdot\text{s}^{-1}$.

electropolymerization of acrylic acid in the presence of ZnCl_2 .⁸ The incorporated Zn metal was washed from the polymer film with HCl, 0.1 M. CdS nanoparticles (5 nm) capped with a mixed monolayer consisting of 3-mercaptopropanesulfonate and cysteamine, to yield a water soluble nanoparticle solution. XPS analysis indicated that ca. 84% of the Cd^{2+} surface groups were linked to the thiolated molecules, and that the ratio between the cysteamine and thiol sulfonate units was ca. 1:10, respectively. The particles were incorporated into the PAA by the “breathing-in” method.^{6,15} By this process the PAA film is shrunk in acetone, and the shrunken film was allowed to swell in the aqueous solution of the CdS nanoparticles. The swelling resulted in the incorporation of the CdS particles into the PAA film. By repeated shrinking/swelling of the PAA film, the content of the CdS nanoparticles increased, and the particles were fixed in the polymer matrix by their entanglement within the cross-linked polymer chains. After five “breathing-in” cycles, the content of the CdS nanoparticles in the polymer film reached a saturation value. To yield an integrated system, the CdS nanoparticles were covalently linked to the carboxylic acid residues of PAA. Microgravimetric quartz crystal microbalance (QCM) measurements indicate that the polymer coverage corresponds to $3.9 \times 10^{-5} \text{ g}\cdot\text{cm}^{-2}$ and the content of the CdS particles is $2.08 \times 10^{-5} \text{ g}\cdot\text{cm}^{-2}$ of the polymer matrix (this translates to ca. 6.59×10^{14} CdS particles in the polymer film). The resulting CdS/PAA film was then reacted with CuSO_4 , 0.1 M, to yield the Cu^{2+} -saturated film. Figure 1 shows the cyclic

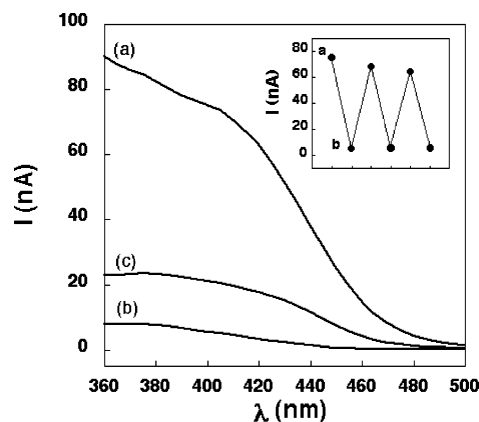
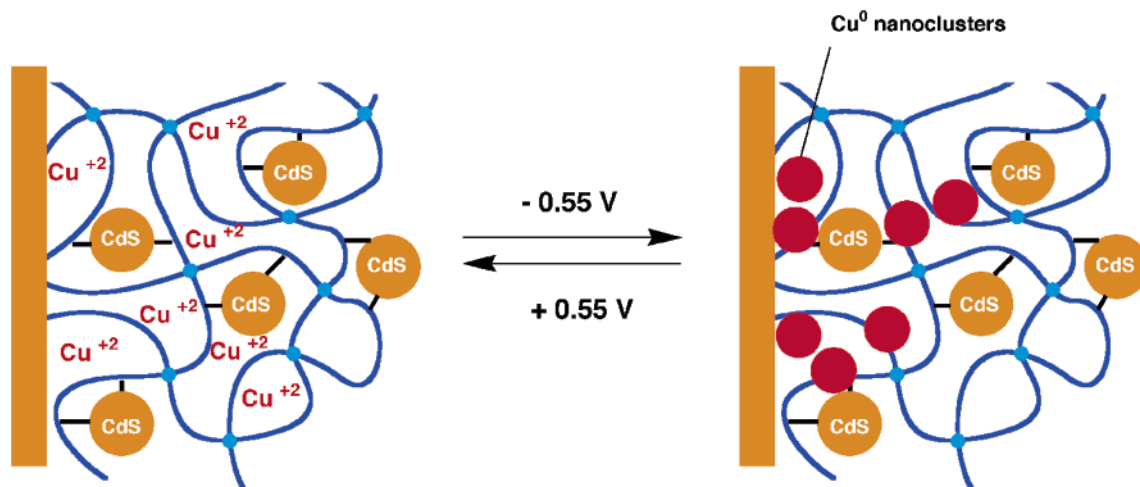


Figure 2. Photocurrent action spectra corresponding to (a) the CdS - Cu^0 -PAA system generated by an applied potential of -0.55 V vs SCE, (b) the CdS - Cu^{2+} -PAA system generated by an applied potential of $+0.55 \text{ V}$ vs SCE, and (c) the CdS -PAA system without the incorporation of Cu^{2+} ions. All systems include 20 mM triethanolamine in 0.1 M Tris buffer solution, pH = 10.0, and irradiation is performed under Ar. Inset: Electroswitchable photocurrents in the CdS - Cu^{2+} -PAA functionalized electrode: (a) applied potential -0.55 V and the formation of the CdS - Cu^0 -PAA state; (b) applied potential $+0.55 \text{ V}$ and the generation of the CdS - Cu^{2+} -PAA state.

voltammogram of the Cu^{2+} -saturated PAA film. At $E < -0.31 \text{ V}$ vs SCE the Cu^{2+} is reduced to Cu^0 , whereas at $E > 0.0 \text{ V}$ vs SCE the Cu metal is redissolved to yield Cu^{2+} linked to the carboxylate residues. By coulometric assay of the Cu^{2+} reduction wave, the Cu^0 content in the film is estimated to be $7.7 \times 10^{-6} \text{ g}\cdot\text{cm}^{-2}$ of the polymer matrix (a similar Cu^0 -content is derived by QCM experiments). XPS measurements indicate that the mass content of Cu^0 in the polymer film is ca. 16%, a value that is in agreement with the QCM analyses.

Figure 2, curve a, shows the photocurrent action spectrum upon applying a potential that corresponds to -0.55 V on the electrode, and upon the irradiation of the system in the presence of triethanol amine, 0.02 M, as sacrificial electron donor. At this applied potential the Cu^{2+} -PAA film is transformed into the metallic Cu^0 -PAA state, Scheme 2. The photocurrent spectrum reveals a shoulder at ca. 410 nm, and it overlaps the absorption spectrum of the CdS nanoparticles. The photocurrent spectrum of the CdS -PAA film upon the application of the potential of 0.55 V, where the Cu^0 is transformed into Cu^{2+} state, is shown in Figure 2, curve b. The photocurrent is completely switched off. Figure 2, curve c shows the photo-

SCHEME 2: Electrochemical Switching of the CdS-Polymer Film between the CdS- Cu^{2+} -PAA and CdS- Cu^0 -PAA States



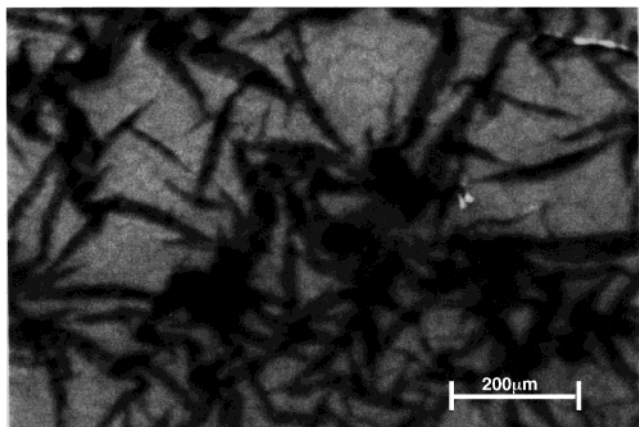


Figure 3. SEM image of the Cu^0 -PAA film.

current spectrum of the CdS-PAA in the absence of Cu^{2+} in the film. The photocurrent spectra of the CdS-PAA system that lacks Cu^{2+} is almost unaffected upon the application of the potentials of +0.55 or -0.55 V on the electrode. Clearly, the electrochemical reduction of the Cu^{2+} to Cu^0 clusters in the CdS-PAA film enhances the photocurrent, and elimination of the Cu^0 clusters yields a 5-fold decrease in the photocurrent. Furthermore, binding of the Cu^{2+} ions to the carboxylate residues of the PAA blocks the low photoelectrochemical activity of the CdS-PAA system. Control experiments reveal that no photocurrent is generated by the Cu^{2+} -PAA or the Cu^0 -PAA films associated with the electrode in the absence of CdS nanoparticles. These results are explained by the fact that the photocurrent originates from the excitation of the CdS nanoparticles that yields an electron-hole pair. The transport of conduction band electrons to the electrode, and the scavenging of the hole by the sacrificial electron donor, lead to the formation of the photocurrent. The electrogeneration of the Cu^0 clusters facilitates the transport of conduction-band electrons by providing conductive sites that trap the electrons and retard the competitive electron-hole recombination. The blocking of the photocurrent in the presence of the Cu^{2+} -carboxylate units is attributed to the quenching of the photoexcited semiconductor nanoparticle and the recombination of the intermediary Cu^+ -hole species. By the cyclic electrochemical switching of the film between the Cu^0 -CdS-PAA and Cu^{2+} -CdS-PAA states, the

photocurrent can be reversibly switched between "ON" and "OFF" states, respectively, Figure 2, inset. Further insight into the conductivity of the Cu^0 -PAA matrix is obtained from the microscopic analysis of the film. Figure 3 shows the SEM image of a cross-section of the film generated upon the reduction of the Cu^{2+} -PAA to the Cu^0 -PAA state. We observe the formation of long Cu^0 wires (length ca. 200 μm , width 2–15 μm) that are in contact with one another. Thus, the Cu^0 wires generate a conductive array that allows the transport of the conduction-band electrons, as suggested by our explanation.

The photocurrents in the $\text{Cu}^0/\text{Cu}^{2+}$ CdS-PAA systems are controlled by the $\text{Cu}^0/\text{Cu}^{2+}$ content in the polymer matrix, and thus the system does not act only as a photoelectrochemical switch but reveals also Cu^{2+} -sensing functions. Figure 4A shows the photocurrents generated by the treatment of the CdS-PAA film-functionalized electrode with variable concentrations of Cu^{2+} and upon applying the potential of -0.55 V vs SCE on the electrode. As the concentration of the Cu^{2+} solution is higher, the photocurrents are enhanced. Thus, as the concentration of Cu^{2+} in the solution is elevated, the content of the carboxylate-bound Cu^{2+} in the film increases, and the content of Cu clusters that facilitate the charge transport increases. Thus, the Cu^{2+} -CdS-PAA film acts not only as an electroswitchable photocurrent switch but is active as a photoelectrochemical sensor for Cu^{2+} in the solution. Figure 4B shows the photocurrent action spectra of the CdS-PAA film treated with different concentrations of Cu^{2+} upon applying the potential of 0.55 V vs SCE on the electrode. The photocurrents decrease as the concentration of Cu^{2+} in the bulk solution increases. At the applied potential, the Cu^{2+} ions are retained in the ionic carboxylate complex in the film. Thus, the elevated content of Cu^{2+} in the film at higher bulk concentrations of Cu^{2+} results in the enhanced quenching of the photoexcited nanoparticles, and the decrease of the photocurrents.

In conclusion, the present study has demonstrated that the incorporation of metal ions (Cu^{2+}) into a CdS-PAA film generates an electroswitchable photoelectrochemically active film. The CdS-PAA film may also be used for the photoelectrochemical sensing of Cu^{2+} ions.

Acknowledgment. This study is supported by the Enrique Berman Foundation, The Hebrew University of Jerusalem.

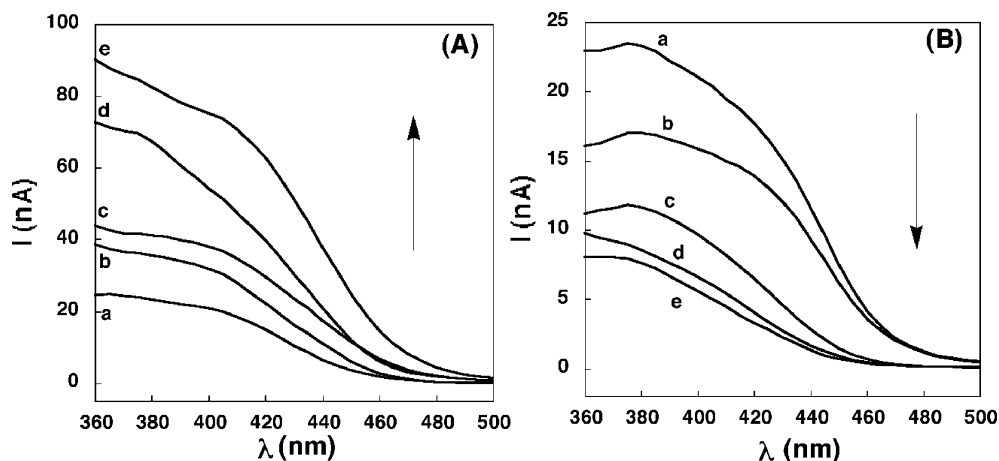


Figure 4. Photocurrent action spectra of the CdS-PAA film treated with different concentrations of Cu^{2+} , upon (A) an applied potential of -0.55 V vs SCE and (B) an applied potential of +0.55 V vs SCE. The concentrations of CuSO_4 in the different experiments correspond to (a) 0 μM , (b) 2 μM , (c) 4 μM , (d) 8 μM , and (e) 10 μM . Data were recorded under the conditions described in Figure 2.

References and Notes

- (1) (a) Shipway, A. N.; Katz, E.; Willner, I. In *Structure and Bonding*; special volume on *Molecular Machines and Motors*; Sauvage, J.-P., Ed.; Springer-Verlag: Berlin, Heidelberg, 2001; Vol. 99, pp 237–281. (b) Liu, Z. F.; Hashimoto, K.; Fujishima, A. *Nature* **1990**, *347*, 658–660.
- (2) (a) Gilat, S. L.; Kawai, S. H.; Lehn, J.-M. *Chem. Eur. J.* **1995**, *1*, 275–284. (b) Kawai, S. H.; Gilat, S. L.; Ponsinet, R.; Lehn, J.-M. *Chem. Eur. J.* **1995**, *1*, 285–293. (c) Doron, A.; Portnoy, M.; Lion-Dagan, M.; Katz, E.; Willner, I. *J. Am. Chem. Soc.* **1996**, *118*, 8937–8944.
- (3) Shipway, A. N.; Willner, I. *Acc. Chem. Res.* **2001**, *34*, 421–432.
- (4) Raitman, O. A.; Katz, E.; Willner, I.; Chegel, V. I.; Popova, G. V. *Angew. Chem., Int. Ed.* **2001**, *40*, 3649–3652.
- (5) Raitman, O. A.; Patolsky, F.; Katz, E.; Willner, I. *Chem. Commun.* **2002**, 1936–1937.
- (6) Pardo-Yissar, V.; Bourenko, T.; Wasserman, J.; Willner, I. *Adv. Mater.* **2002**, *14*, 670–673.
- (7) Pardo-Yissar, V.; Katz, E.; Wasserman, J.; Willner, I. *J. Am. Chem. Soc.* **2003**, *125*, 622–623.
- (8) Chegel, V. I.; Raitman, O. A.; Lioubashevski, O.; Shirshov, Y.; Katz, E.; Willner, I. *Adv. Mater.* **2002**, *14*, 1549–1553.
- (9) Katz, E.; Willner, I. *J. Am. Chem. Soc.* **2003**, *125*, 6803–6813.
- (10) (a) Sabramanian, V.; Wolf, E.; Kamat, P. V. *J. Phys. Chem. B* **2001**, *105*, 11439–11446. (b) Kamat, P. V.; Shanghavi, B. *J. Phys. Chem. B* **1997**, *39*, 7675–7679.
- (11) (a) Nasr, C.; Hotchandani, S.; Kim, W. Y.; Schenehl, R. H.; Kamat, P. V. *J. Phys. Chem. B* **1997**, *101*, 7480–7487. (b) Sant, P. A.; Kamat, P. V. *Phys. Chem. Chem. Phys.* **2002**, *4*, 198–203.
- (12) Buttry, D. A.; Ward, M. D. *Chem. Rev.* **1992**, *92*, 1355–1379.
- (13) Miyake, M.; Matsumoto, H.; Nishizawa, M.; Sakata, T.; Mori, H.; Kuwabata, S.; Yoneyama, H. *Langmuir* **1997**, *13*, 742–746.
- (14) Katz, E.; DeLacey, A. L.; Fernandez, V. M. *J. Electroanal. Chem.* **1993**, *353*, 261–272.
- (15) (a) Pardo-Yissar, V.; Gabai, R.; Shipway, A. N.; Bourenko, T.; Willner, I. *Adv. Mater.* **2001**, *13*, 1320–1323. (b) Sheeney-Haj-Idia, L.; Sharabi, G.; Willner, I. *Adv. Funct. Mater.* **2002**, *12*, 27–32.